Title
HEAVY-PARTICLE STUDIES WITH SILICON DETECTORS

Author
Raju, Mudundi R.

Publication Date
1965-08-20

UCRL-16354

University of California

Ernest O. Lawrence Radiation Laboratory

HEAVY-PARTICLE STUDIES WITH SILICON DETECTORS

Berkeley, California

Submitted for presentation in the
Work Shop Conference on Space
Radiation Biology—Berkeley, Calif.
Sept. 7–10, 1965.
(Proceedings)—Radiation Research

UCRL-16354

UNIVERSITY OF CALIFORNIA

Lawrence Radiation Laboratory
Berkeley, California

AEC Contract No. W-7405-eng-48

HEAVY-PARTICLE STUDIES WITH SILICON DETECTORS

Mudundi R. Raju

August 20, 1965

Proposed running head:

Si DETECTORS FOR HEAVY PARTICLES

Mailing address:

Mudundi R. Raju

Donner Laboratory and Donner Pavilion

Lawrence Radiation Laboratory

University of California

Berkeley, California 94720

Heavy-Particle Studies with Silicon Detectors

Mudundi R. Raju

Donner Laboratory and Donner Pavilion
Lawrence Radiation Laboratory
University of California
Berkeley, California

August 20, 1965

INTRODUCTION

The response of lithium-drifted silicon detectors is studied with a view to determining applications of these detectors to radiobiologic problems. Until recently these detectors had only limited applications because they were available only with limited thickness. Now the technology has been improved and detectors several mm thick are available (see reference 1, for example). The availability of these detectors has revolutionized radiation detection and spectroscopy (2). The use of a solid as a detector is very atrractive, because the sensitive layer can be quite thin and yet possess a high stopping power. Another advantage results from the low energy to produce one hole-electron pair (3.6 eV in silicon): nearly ten times as much charge is produced for a given energy loss in silicon as in gas, which leads to small statistical fluctuations in the number of pairs and improved energy resolution over gas-filled counters. The intrinsically high speed of the device is due to the high mobility of the carriers in the electric field, coupled with the short distance between electrodes.

An attractive feature of these detectors is that they operate as true energy devices, and do not exhibit saturation effects as do scintillation counters.

Depending on the energy of the particles and the thickness of the detector, a given detector may be used to measure either their energy-loss distribution or energy distribution. If the detector thickness is small, so that the energy deposited by the particle in it is very small compared with the energy of the particles, it can be used to measure the energy-loss distribution. On the other hand, if the detector is thick enough to stop all the particles in the beam, then it can be used to measure energy distribution of the particles.

The use of these detectors for the study of pion beams and to measure the pion-star energy distribution in silicon has been reported(3). Also, the application of these detectors to experimentally verify the Landau theory of energy-loss distribution has been reported(4).

In this investigation the response of these detectors to high-energy alpha and proton beams, and the intermediate energies obtained by placing absorbing materials in the path of the primary beam, have been studied.

The Bragg peak of heavy particles is often used for therapy and for radiobiological investigations. Besides knowing the dose at the Bragg peak position, one should also know the LET distribution at this position. In order to evaluate the LET distribution of heavy particles at the Bragg peak position, the energy distribution of these particles is measured.

CALIBRATION

The experimental setup is shown in Fig. 1. The test-pulse generator is used to simulate detector pulses and to check the linearity of the electronic system.

An Am^{241} alpha source and a Bi^{207} internal conversion electron source are used for calibrating the pulse-generator output in terms of energy. Calibration and linearity checks are made for every experiment.

RESULTS

Beam: Helium Nuclei

The Berkeley heavy-ion linear accelerator (Hilac) accelerates nuclei to an energy of 10.40± 0.2 MeV per nucleon. For helium nuclei the energy of the primary beam is 41.6 MeV. The beam comes out through a vacuum column with a 1-mil aluminum window. The detector is enclosed by a housing (in order that a vacuum can be maintained) with a 1-mil Mylar window. The entire detector holder assembly is surrounded with a 1/4-mil aluminum electronic shield. By applying the correction for the degradation of the energy of the primary beam through these foils, one finds the energy of the beam seen by the detector to be 40.0 MeV. The lower energies of the α particles are obtained by putting standard aluminum absorbers in the beam.

A 1-mm-thick lithium-drifted silicon detector is used for this beam. The energy of the α particles that corresponds to the range in 1-mm silicon is about 50 MeV. Hence this beam can be stopped in the detector. The spectral response of the energy absorbed in the detector from the corrected primary beam of 40 MeV is shown in Fig. 2. The energy of the beam obtained from calibration is 39.88 MeV, which agrees very well with the corrected primary energy of 40 MeV. When a particle is stopped in a detector, the resolution is a function of the detector and the electronic system. Values for full width at half maximum (FWHM) from 2 keV upwards (depending upon the type of experiment) have been obtained by many workers with semiconductor detectors exposed to monoenergetic particles, giving resolutions much less than 1%. FWHM obtained in this measurement is 0.62 MeV, giving a resolution of 1.5% (when the detector is operated at room temperature). This poorer resolution is partly due to momentum spread of the beam.

However, better resolutions can be obtained by operating the detector at low temperature.

The spectra of different low-energy α particles obtained by degrading the primary beam by aluminum absorbers are also shown in Fig. 2 and the results are tabulated in Table I. The agreement between the residual energies calculated by using range-energy tables (5) and the experimental values is good. The α particles emerging from the absorbing material, especially when the absorbers are thick, had a wider energy spread than the primary beam. This can be seen clearly in Fig. 2. This wider spread is due to small-angle scattering and energy straggling.

<u>Beam: 910-MeV Alpha Particles</u>

The Berkeley 184-inch synchrocyclotron accelerates α particles to 910 MeV and protons to 732 MeV. The response of a 0.48-gm/cm^2 lithium-drifted silicon detector to α particles of 910 MeV and lower energies is investigated. At high energies the detectors would operate as dE/dx detectors. The width of a peak is determined by many factors in addition to those imposed by the electron system. Slight variations in path length, i. e., internal scattering, produce a spread in the energy absorbed. So do statistical fluctuations in the energy transfer in inelastic collision processes. Hence, particles of originally the same energy may produce measurably different signals, causing a spread of the energy loss spectrum.

Since the charge collected from a detector is proportional to the loss of energy by the incident particle in the sensitive region, α particles, which are totally absorbed in this region, produce corresponding pulses of larger amplitude than α particles of higher energy, which pass completely through. For monoenergetic α particles whose range is greater than the depth of the depletion region, the charge-pulse amplitude from the detector increases with decreasing alpha energy until the range of α particles in silicon equals the sensitive depth. A further decrease in alpha energy causes a proportional decrease in the charge pulse.

The thickness of the detector depletion layer determines the measured energy loss. In our case, the depletion layer extends almost through the entire physical thickness of the detector except for a few mils on the lithium side. The method used to measure this depletion thickness is to determine the maximum energy deposited in the detector. The range of the α particle in silicon whose energy corresponds to this maximum energy is then obtained from range-energy tables (5).

The response of the detector for the 910-MeV beam and for the beam degraded by using copper absorbers is shown in Figs. 3 and 4. As we increased the thickness of the copper absorber in the beam, the energy of the α particles would be lowered and hence the dE/dx would increase, with a concomitant increase in the energy spread. The experimental and theoretical values of energy loss shown in Table II are in close agreement down to a residual energy of 330 MeV. At lower energies this agreement is lacking, because at these energies the detector is not a dE/dx detector. If we estimate the energy deposited in the detector at these lower energies, instead of dE/dx, a good agreement can be obtained. Experiments with detectors of thicknesses 1/4, 1, 3, and 5 mm also gave good agreement with theoretical values of dE/dx.

The Bragg peak obtained by use of ionization chambers is at 2.10 in. of copper. The response of the detector at the Bragg peak position is also shown in Fig. 4b. The maximum energy that can be deposited in the detector is due to the particles that have a range in Li equal to the thickness of the depletion layer. In this experiment the maximum cutoff energy is 73 MeV. The corresponding range in silicon, from range-energy tables (5), is 0.48 gm/cm^2. The physical thickness of the detector as determined with a micrometer is about 5% greater than this value. This difference is due to the dead layer on the Li side. The experimental accuracy in the determination of detector thickness is within about 2%.

It appears from these data that the energy spectrum of the α particles at the Bragg peak position extends to more than 75 MeV. This detector (0.48 gm/cm^2) at this position is neither dE/dx nor total-energy type. The small hump in Fig. 4b is due to the particles of energy higher than 73 MeV passing through the detector and hence depositing less energy. This hump vanished when the beam was degraded further by copper absorbers. As a rough estimate, 1/4-mm-thick detector can be considered as dE/dx detector at the Bragg peak position. The response of this detector at the Bragg peak position is shown in Fig. 5. The energy loss in the detector is 4.8 MeV, FWHM 2.97 MeV. The energy of the alpha beam corresponding to this energy deposition is 80 MeV and, at 50% level, 54 and 103 MeV. Thus we can roughly estimate that the energy spectrum of the alpha beam at the Bragg peak position is mostly in the region 54 to 103 MeV, with an average value around 80 MeV.

The energy distribution at the Bragg peak position can be obtained very accurately by using a detector thick enough to stop all the particles. A 5-mm-thick detector can stop α particles of energy 120 MeV. Figure 6 shows the energy distribution of α particles at the Bragg peak position with a 5-mm-thick detector. It can be seen from the figure that the average energy of the α particles at the Bragg position is 85 MeV. These data can be translated into LET distribution, which is shown in the same figure; the average LET is around 10 keV/μ.

Beam: 49-MeV Protons

Berkeley's 88-inch cyclotron accelerates protons up to 50 MeV and α particles up to 120 MeV. Figure 7 shows the response of 0.68-gm/cm^2 detector for 49-MeV protons. The energy loss in the detector is in good agreement with the theoretical value. The Bragg peak for the 49-MeV proton beam is obtained at 2.58 gm/cm^2 of aluminum. Figure 8 shows the energy distribution of protons at this Bragg peak position. It can be seen from the figure that the average energy of the proton is around 5 MeV. Corresponding LET values are also shown in the figure, the average LET being around 8 keV/μ.

SUMMARY

The lithium-drifted silicon semiconductor detectors used in this study of high-energy α particles and protons give very promising results in measuring energy loss and energy distribution. Indeed, the agreement between the theoretical and experimental values of residual energy and energy loss is very good. The energy distribution at the Bragg peak positions of 910-MeV alpha beam and 49-MeV proton beam is measured in order to evaluate the LET distribution at the Bragg peak.

From the data it seems that the average energy of the heavy particles at the Bragg peak position is roughly 10% of the primary beam energy.

ACKNOWLEDGMENTS

I wish to thank Professor John H. Lawrence and Professor Cornelius A. Tobias for their encouragement. Special thanks to Donald A. Landis, Robert Lothrop and Harry E. Smith for supplying the detectors and helpful discussions on their use. Also, the discussions with Fred Goulding, Dr. John T. Lyman, and Dr. Henry Aceto, Jr., are most appreciated.

This work was done under the auspices of the U. S. Atomic Energy Commission and the National Aeronautics and Space Administration.

REFERENCES

1. F. Goulding. A survey of the applications and limitations of various types of detectors in radiation energy measurement. IEEE Trans. Nucl. Sci., Vol. NS-11 [3], 177–190, 1964.
2. Solid State Radiation Detectors, various articles in IRE Trans. Nucl. Sci. 8 (Jan. 1961).
3. M. R. Raju, H. Aceto, and C. Richman. Pion studies with silicon detectors. Nucl. Instr. and Methods (to be published).
4. H. D. Maccabee and M. R. Raju. Fluctuations of energy loss by charged particles in silicon detectors, Nucl. Instr. and Methods (to be published).
5. L. Williamson and J. P. Boujot. Tables of range and rate of energy loss of charged particles of energy 0.5 to 150 MeV. Centre d'Etudes Nucléaires de Saclay, 1962.

Table I. 40-MeV α beam in 1-mm silicon detector.

Al absorber (mg/cm^2)	Residual energy (MeV) Calc.	Residual energy (MeV) Expt.
0	40.00	39.88
15.2	37.90	37.71
29.9	35.71	35.67
44.5	33.53	33.39
59.8	31.16	31.01
75.0	28.63	28.42
89.7	25.96	25.67
104.5	23.05	22.68
134.2	15.59	15.37
155.2	9.17	8.67

Table II. 910-MeV α beam in 0.48-gm/sec^2 silicon detector.

Cu absorber thickness (in.)	Residual energy (MeV)	Energy loss (MeV) Theory	Energy loss (MeV) Expt.
0	910	6.44	6.38
0.493	775	7.10	7.07
1.001	620	8.25	8.28
1.495	440	10.49	10.58
1.755	330	12.92	13.35
2.002	175	20.90	23.10

FIGURE LEGENDS

Fig. 1. Experimental setup.

Fig. 2. Response of 1-mm detector to 40-MeV α beam and the beam degraded by

(a) 89.7 and 134.2 mg/cm^2 Al,

(b) 155.2-mg/cm^2 Al.

Fig. 3. Response of 0.48-gm/cm^2 (≈ 2mm) detector to 910-MeV α beam, and the beam degraded by 1.495 in. cu.

Fig. 4. Response of 0.48-gm/cm^2 (≈ 2mm) detector to 910-MeV α beam degraded by

(a) 2.002 in. cu.,

(b) 2.100 in. cu (Bragg peak).

Fig. 5. Response of 1/4-mm detector to 910-MeV α beam at the Bragg peak position.

Fig. 6. Distribution of α-particle energy at the Bragg peak position of 910-MeV α beam.

Fig. 7. Response of 0.68 gm/cm^2 (≈ 3mm) detector to 49-MeV proton beam.

Fig. 8. Energy distribution at the Bragg peak position of 49-MeV proton beam.

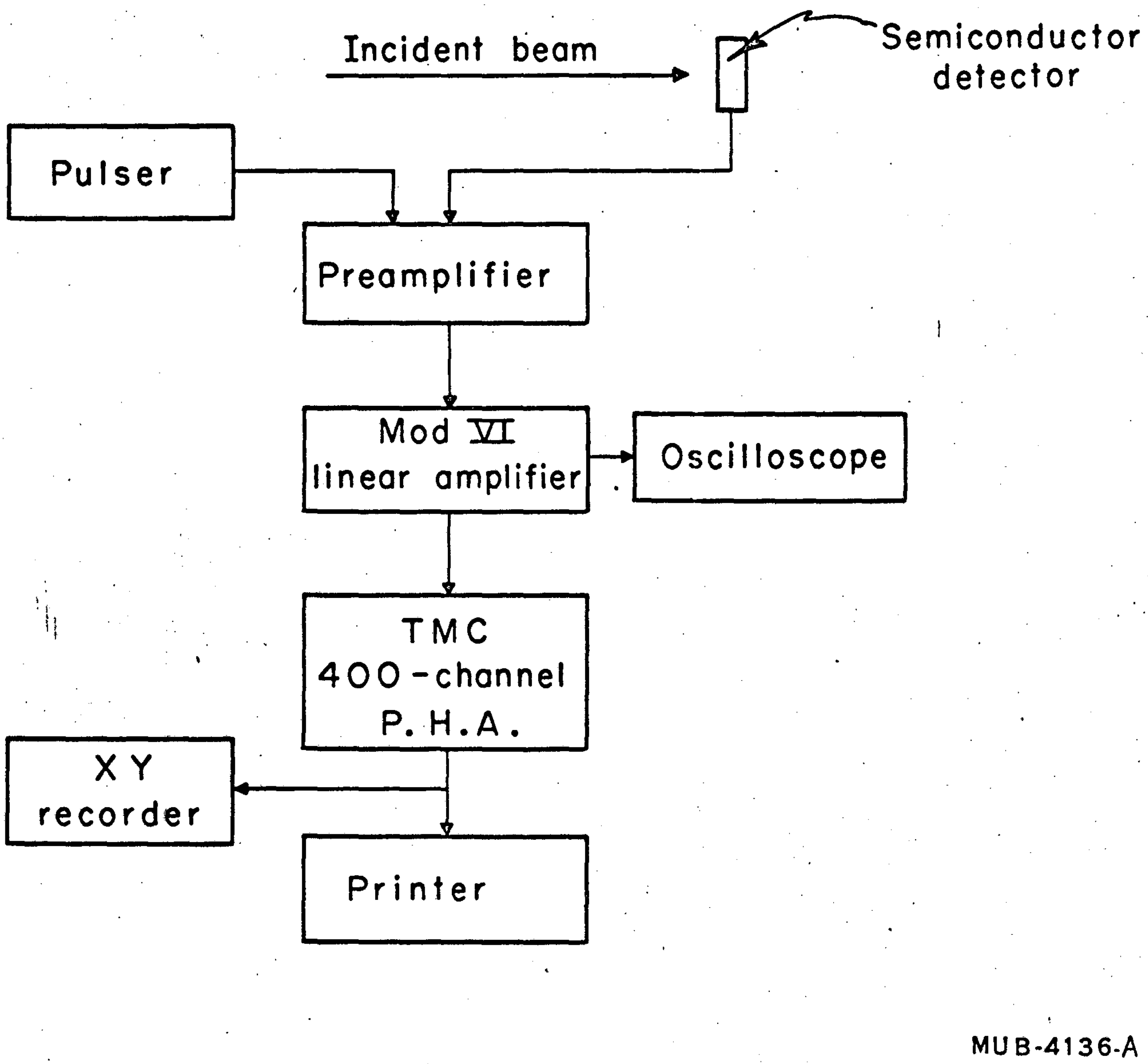
Incident beam
Semiconductor detector
Pulser
Preamplifier
Mod VI linear amplifier
Oscilloscope
TMC 400-channel P.H.A.
X Y recorder
Printer
MUB-4136-A

Fig. 1.

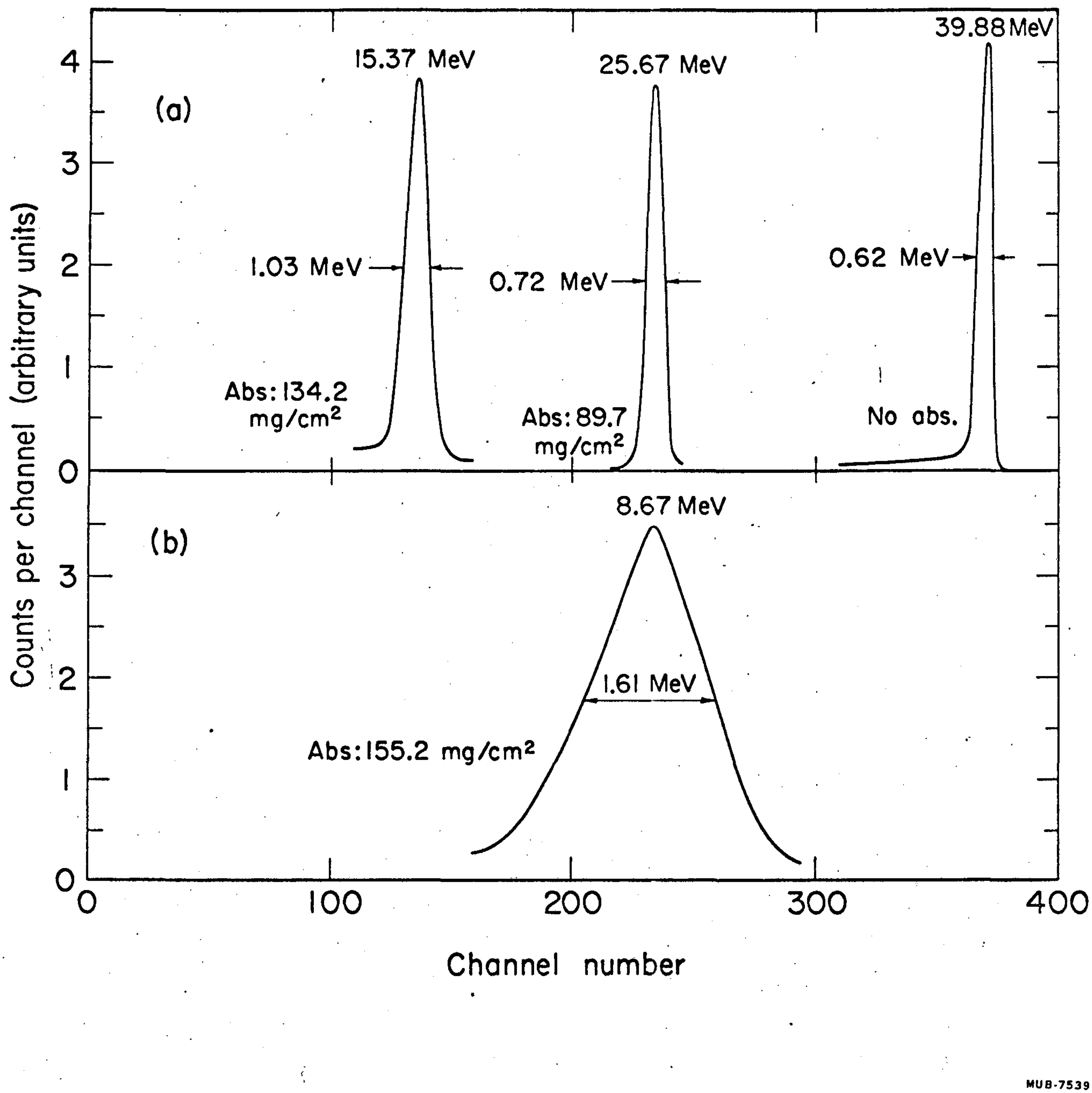
15.37 MeV
25.67 MeV
39.88 MeV
(a)
1.03 MeV
0.72 MeV
0.62 MeV
Abs: 134.2 mg/cm²
Abs: 89.7 mg/cm²
No abs.
8.67 MeV
(b)
1.61 MeV
Abs: 155.2 mg/cm²
Counts per channel (arbitrary units)
Channel number
MUB-7539

Fig. 2.

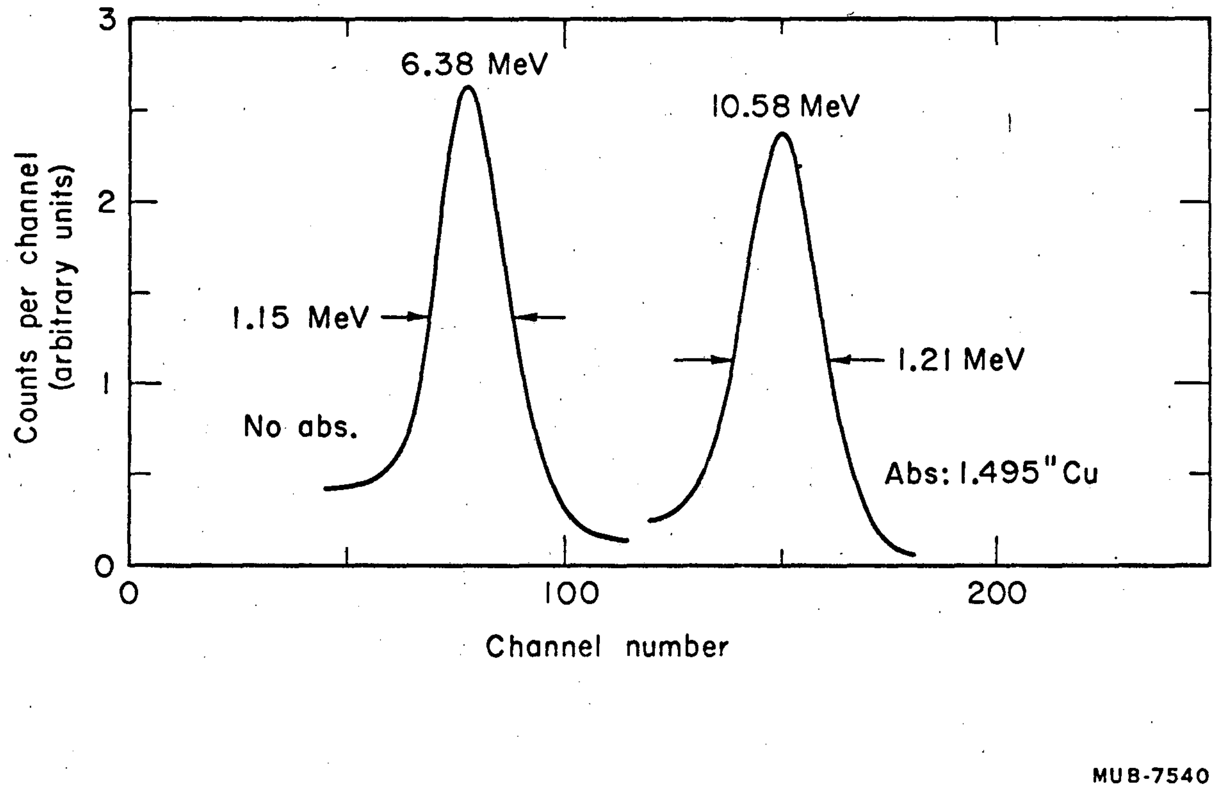
6.38 MeV
10.58 MeV
1.15 MeV
1.21 MeV
No abs.
Abs: 1.495" Cu
Counts per channel (arbitrary units)
Channel number
0
1
2
3
0
100
200
MUB-7540

Fig. 3.

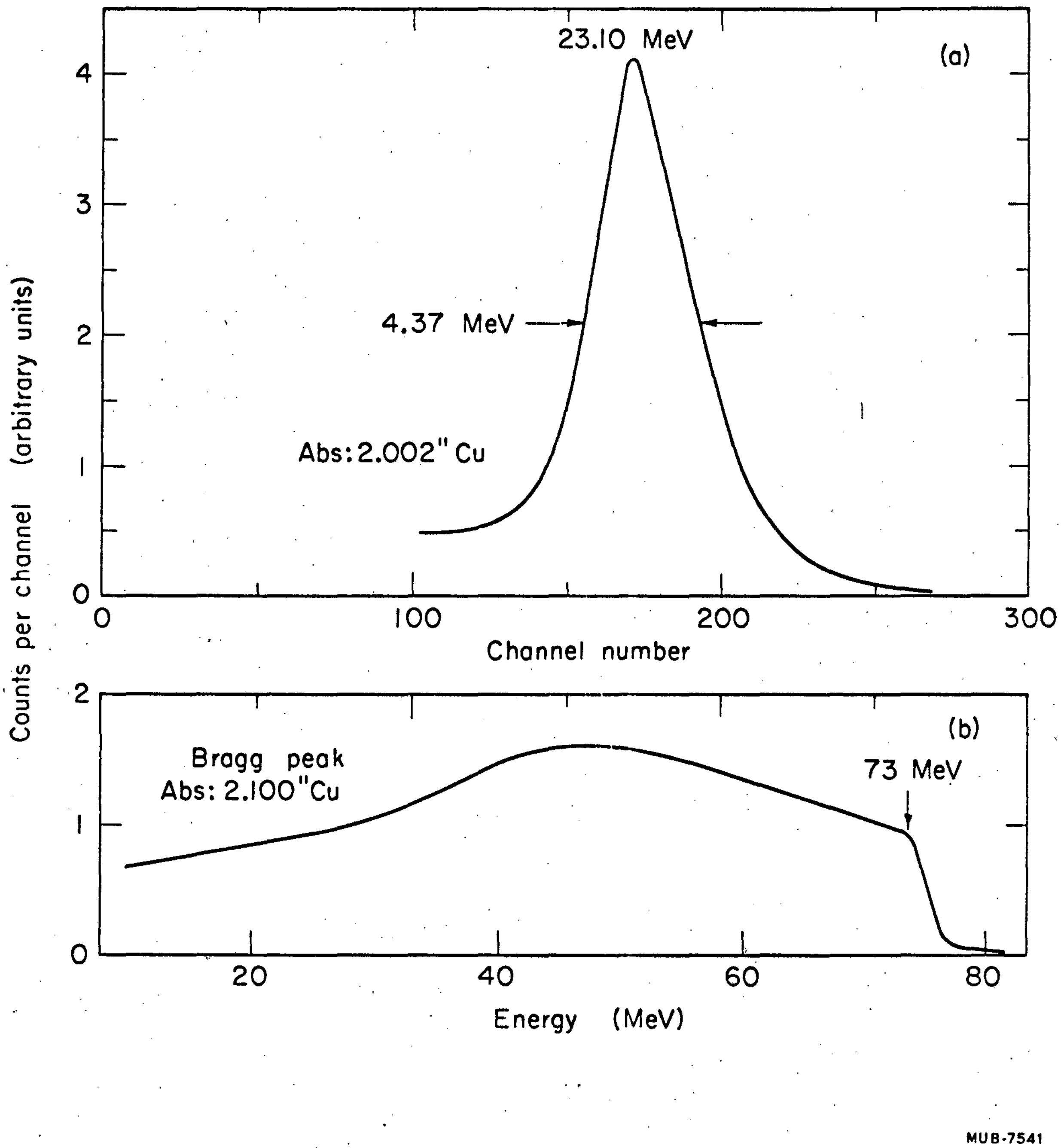
23.10 MeV
(a)
4.37 MeV
Abs: 2.002" Cu
Counts per channel (arbitrary units)
Channel number
(b)
Bragg peak
Abs: 2.100" Cu
73 MeV
Energy (MeV)
MUB-7541

Fig. 4.

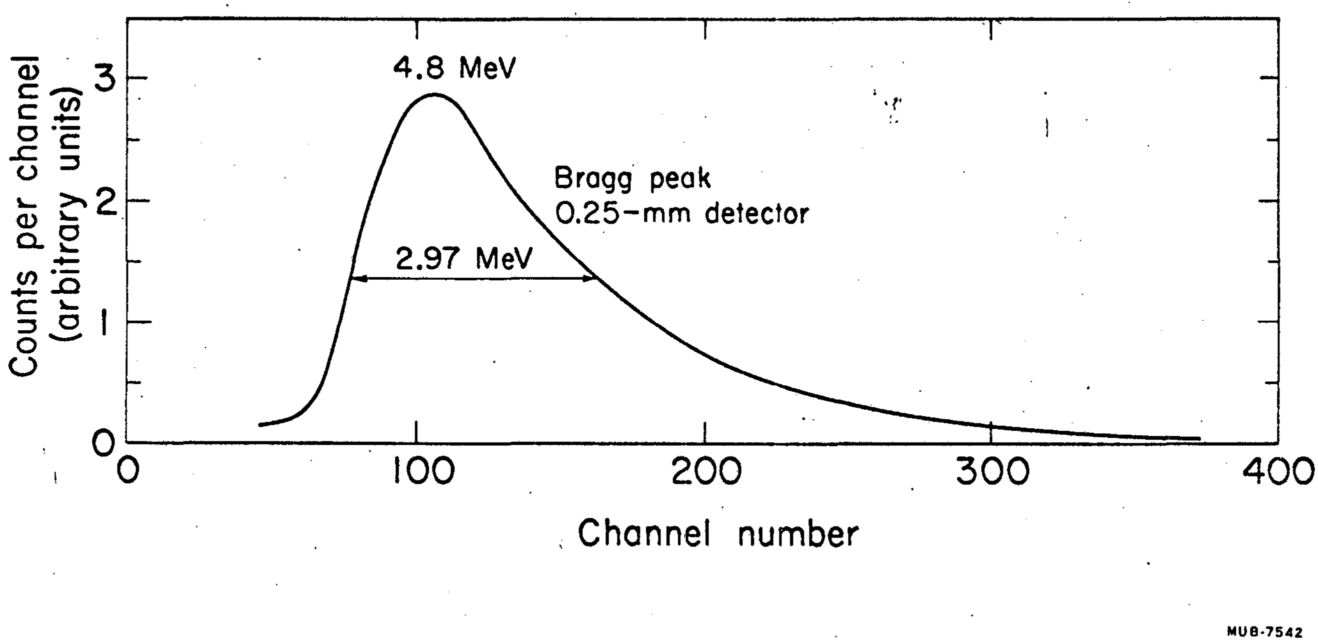
Counts per channel
(arbitrary units)
4.8 MeV
Bragg peak
0.25-mm detector
2.97 MeV
0
1
2
3
0
100
200
300
400
Channel number
MUB-7542

Fig. 5.

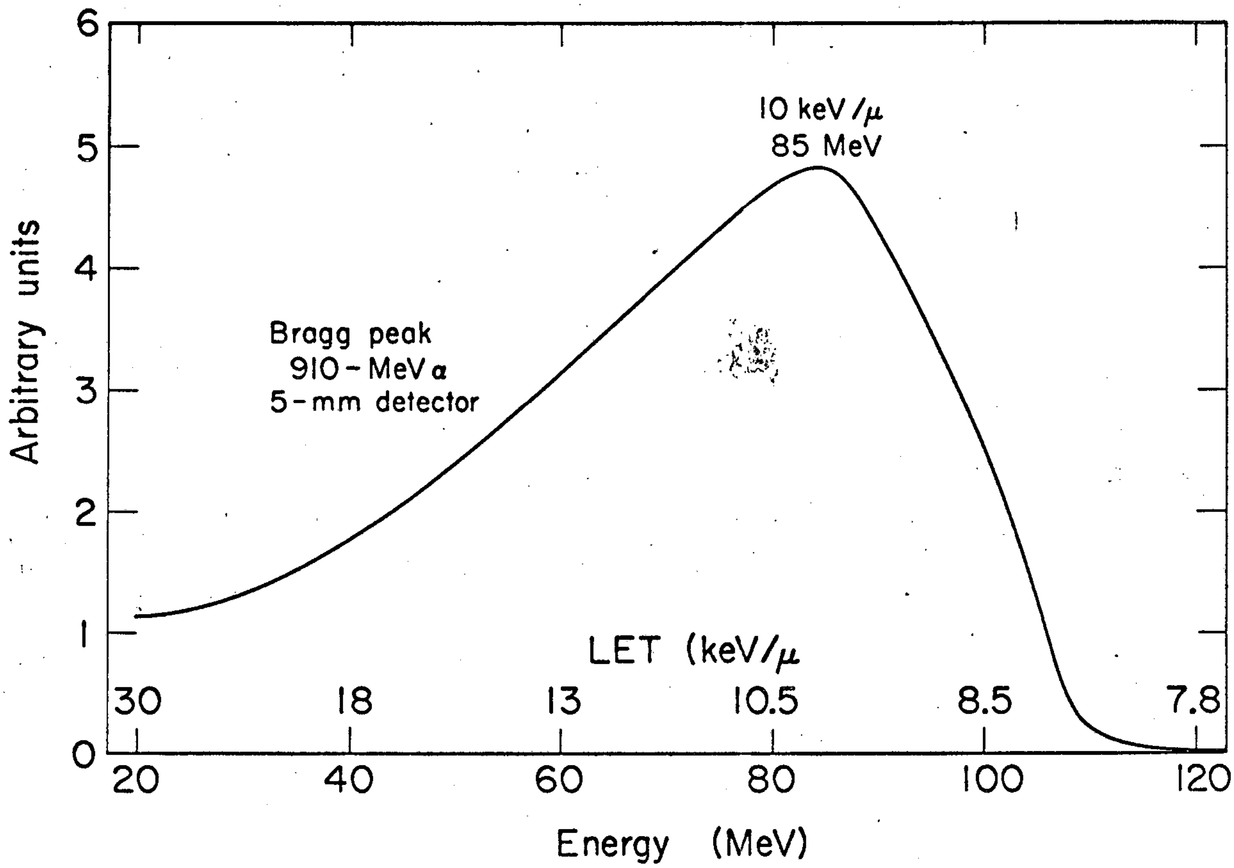

MUB-7543

Fig. 6.

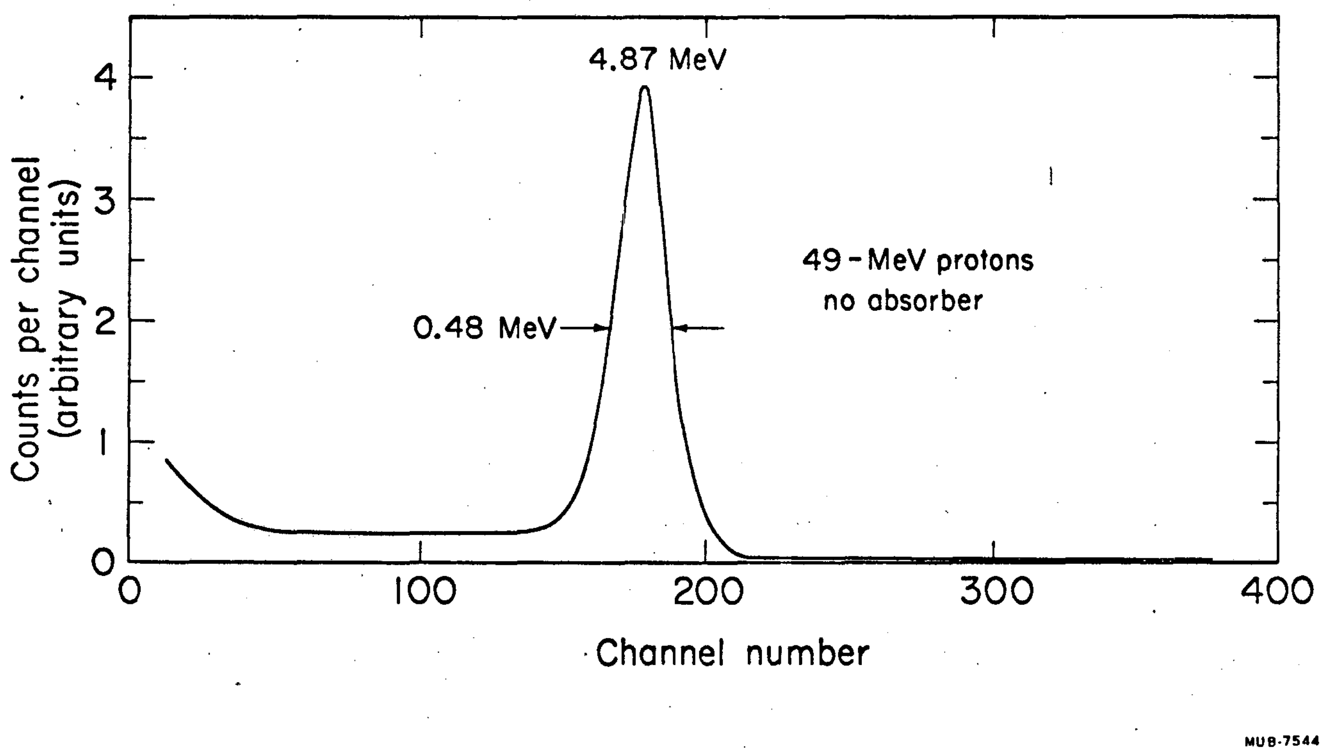
4.87 MeV
49 - MeV protons
no absorber
0.48 MeV
Counts per channel
(arbitrary units)
Channel number
0
1
2
3
4
0
100
200
300
400
MUB-7544

Fig. 7.

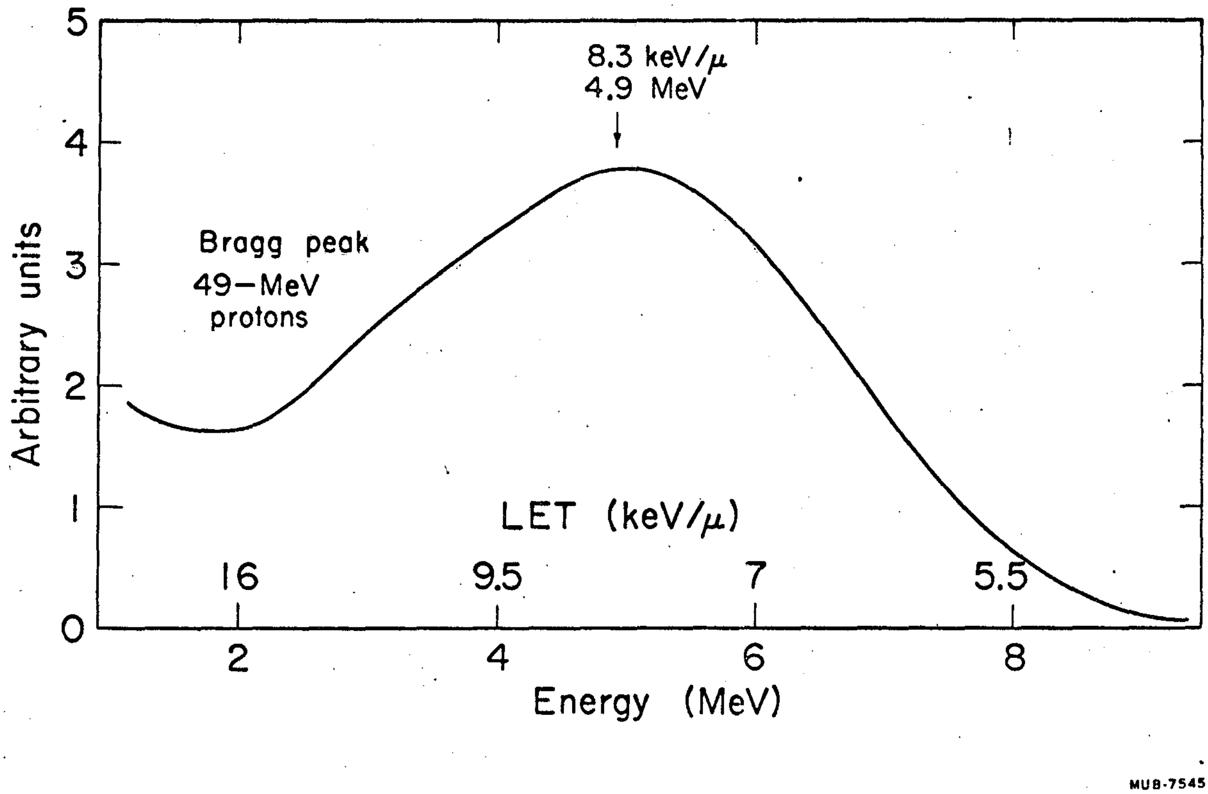
5
4
3
2
1
0
Arbitrary units
8.3 keV/μ
4.9 MeV
Bragg peak
49-MeV
protons
LET (keV/μ)
16
9.5
7
5.5
2
4
6
8
Energy (MeV)
MUB-7545

Fig. 8.